Computed Tomography Characteristics Predictive for Radial EBUS-Miniprobe-Guided Diagnosis of Pulmonary Lesions

Canan Guvenc, Msc, Jonas Yserbyt, MD,† Dries Testelmans, MD, PhD,† Federica Zanca, PhD,‡ An Carbonez, PhD,§ Vincent Ninane, MD, PhD,† Walter De Wever, MD, PhD,* and Christophe Dooms, MD, PhD†*

Introduction: Radial endobronchial ultrasonography miniprobe (rEBUS-MP) is a technique that has increased the diagnostic yield of bronchoscopic occult pulmonary lesions. The purpose of this study was to identify computed tomography (CT) characteristics affecting the success rate of rEBUS-MP in the evaluation of these pulmonary lesions.

Methods: Our study encompassed a retrospective review of all consecutive patients who underwent a rEBUS-MP examination between January 2011 and December 2013. CT characteristics including lesion size, lesion location, and bronchus sign were analyzed against two defined outcomes (visualization yield and diagnostic yield). Univariate analysis was employed to examine the individual effects of each CT parameter on visualization yield and diagnostic yield. Multivariate logistic regression was performed to identify significant predictors of diagnostic yield.

Results: Seven hundred and sixty lesions (760 patients) were included. The mean ± SD longest lesion diameter was 43 ± 2 mm. rEBUS-MP could visualize 83% and a definitive diagnosis was established in 62%. In a multivariate analysis, longest lesion diameter greater than 20 mm (odds ratio [OR]: 1.97 and $p = 0.036$), distance lesion to secondary or tertiary carina greater than 40 mm (OR: 0.60 and $p=0.016$), and lobar segment (1, 3, or 6, respectively) were determined to be significant factors predicting diagnostic yield. Bronchus sign was the only parameter that indirectly influenced the diagnostic yield through enhancing visualization yield ($p < 0.001$).

Conclusion: Multivariate analysis revealed that lesion size, distance to carina, and segment were predictors of diagnostic yield. The presence of a bronchus sign substantially increased the diagnostic yield through the visualization yield.

Key Words: Diagnosis, Pulmonary lesion, Radial endobronchial ultrasonography.

(*J Thorac Oncol.* 2015;10: 472–478)

*Department of Radiology, University Hospitals KU Leuven, 3000 Leuven, Belgium; †Respiratory Division, University Hospitals KU Leuven, 3000 Leuven, Belgium; ‡Department of Imaging and Pathology, University Hospitals KU Leuven, 3000 Leuven, Belgium; and §Leuven Statistics Research Centre, KU Leuven, 3000 Leuven, Belgium.

Disclosure: The authors declare no conflict of interest.

Address for Correspondence: Christophe Dooms, MD, PhD, Respiratory Division, University Hospitals KU Leuven, Herestraat 49, B-3000 Leuven. E-mail: christophe.dooms@uzleuven.be

DOI: 10.1097/JTO.0000000000000410

ISSN: 1556-0864/15/1003-0472

The diagnosis of a pulmonary lesion that is present beyond the endoscopically visualized bronchi using a conventional flexible videobronchoscope (outer diameter 5–6 mm) is clinically challenging[1–2]. Advances in bronchoscopic and navigation techniques have allowed clinicians to provide a continued increase in the diagnostic yield of the endoscopic procedure. The assessment of pulmonary lesions consists of the manual inspection of multidetector computed tomography (CT) images to establish a mentally driven route toward the lesion followed by a live bronchoscopy with radial endobronchial ultrasound miniprobe (rEBUS-MP) to approach endoscopically occult pulmonary lesions. A recent meta-analysis reported a diagnostic yield of 71% (95% confidence interval [CI]: 67–76%) for bronchoscopy with rEBUS-MP-guided transbronchial lung biopsy (TBLB) of endoscopically occult pulmonary lesions [3]. The complication rate of this rEBUS-MP-guided TBLB is extremely low as compared with traditional transthoracic needle biopsy or surgical sampling techniques, with a pooled rate of chest drainage for pneumothorax of only 0.4%[4]. Other new guided bronchoscopy techniques, such as electromagnetic navigation, virtual bronchoscopic navigation, and ultrathin bronchoscopy reach a similar diagnostic yield of approximately 70%[3,5]. Apart from the effects of operational differences at various institutions, the diagnostic yield of these new technologies is considerably affected by CT characteristics of the investigated pulmonary lesion.[6–10] The consequence might be that the diagnostic method to reach and biopsy a pulmonary lesion could be based on lesion location, lesion size, and/or expertise available.

We designed a retrospective study to evaluate the CT characteristics that might influence the diagnostic yield of EBUS-MP-guided TBLB of a pulmonary lesion and to propose an algorithm to approach an endoscopic occult parenchymal pulmonary lesion.

PATIENTS AND METHODS

Patients

Between January 1, 2011 and December 31, 2013, 760 patients with an endoscopically invisible pulmonary lesion underwent an EBUS procedure with a radial ultrasonic miniprobe for diagnostic purpose in a single center. Exclusion criteria for a rEBUS-MP procedure consisted of suspected bronchopneumonia, solid lesions less than 10 mm largest diameter calculated on lung windows from axial CT images, ground

glass opacity (pure or part-solid less than 50%) lesions, and solid lesions less than 15 mm largest diameter touching the visceral pleura. The institutional review board of University Hospitals KU Leuven approved this retrospective study (S56813).

CT analysis

The CT images of these 760 patients were retrospectively reviewed. All CT examinations were made with 64 slice multidetector CT scanners (Siemens, Germany; Philips, The Netherlands) using a standardized contrast-enhanced imaging protocol. Patients were scanned in the supine position in craniocaudal direction at end-inspiration. The scan parameters were as follows: 120 kVp, 85 mAs, and 1 mm scanning thickness. The axial images (5 mm thickness) and coronal images (3 mm thickness) were reconstructed using B30f kernel for mediastinal algorithm and B50f kernel for lung algorithm. Images were transferred to a PACS workstation (AGFA) and IMPAX Volume viewing 3.0 software (AGFA HealthCare NV, Mortsel, Belgium) was used for analysis. CT images were evaluated for the presence of bronchus sign, lesion size, and lesion location. A bronchus sign is the finding on cross-section of a bronchus leading directly to or contained within a nodule or mass[11]. Measurements were performed on lung window settings. First, we identified on axial CT images (Fig. 1*A*) the longest lesion diameter (LLD) and the longest perpendicular lesion diameter (LPLD), and thereafter on coronal CT images (Fig. 1*B*) the largest apicocaudal diameter (LAD). Location of the lesion within the lung was determined by lobe, lobar segment, and by measuring the distance between the lesion and the secondary (for right upper lobe, left upper lobe, and left lower lobe) or tertiary (for right middle lobe and right lower lobe) carina (Dcarina) using IMPAX volume viewing software (Fig. 1*C*). The distance from lesion to the chest wall (Dthorax) was measured on axial CT images as the shortest distance between the lesion and the chest wall (Fig. 1*A*).

Bronchoscopy.

After informed consent videobronchoscopy was performed using an Olympus BF-1T160 or BF-160 with outer diameter 5.2–6.0 mm and working channel 2.0–2.8 mm or a Fujinon EB-530T or EB-530S with outer diameter 4.9–5.8 mm and working channel 2.0–2.8 mm, which can visualize up to fourth- to sixth-order of bronchi. Whenever no lesion was present within the endoscopically visualized bronchi, endobronchial ultrasonography was performed using an endobronchial ultrasound system (processor EU-M20 and driving unit MH-240; Olympus, Japan) equipped with a 20-MHz mechanical radial miniprobe (UM-S20-20R; Olympus). The bronchoscopist inspected in advance the axial and coronal CT scan images to establish a mentally driven route toward the lesion. During bronchoscopy, the lesion was

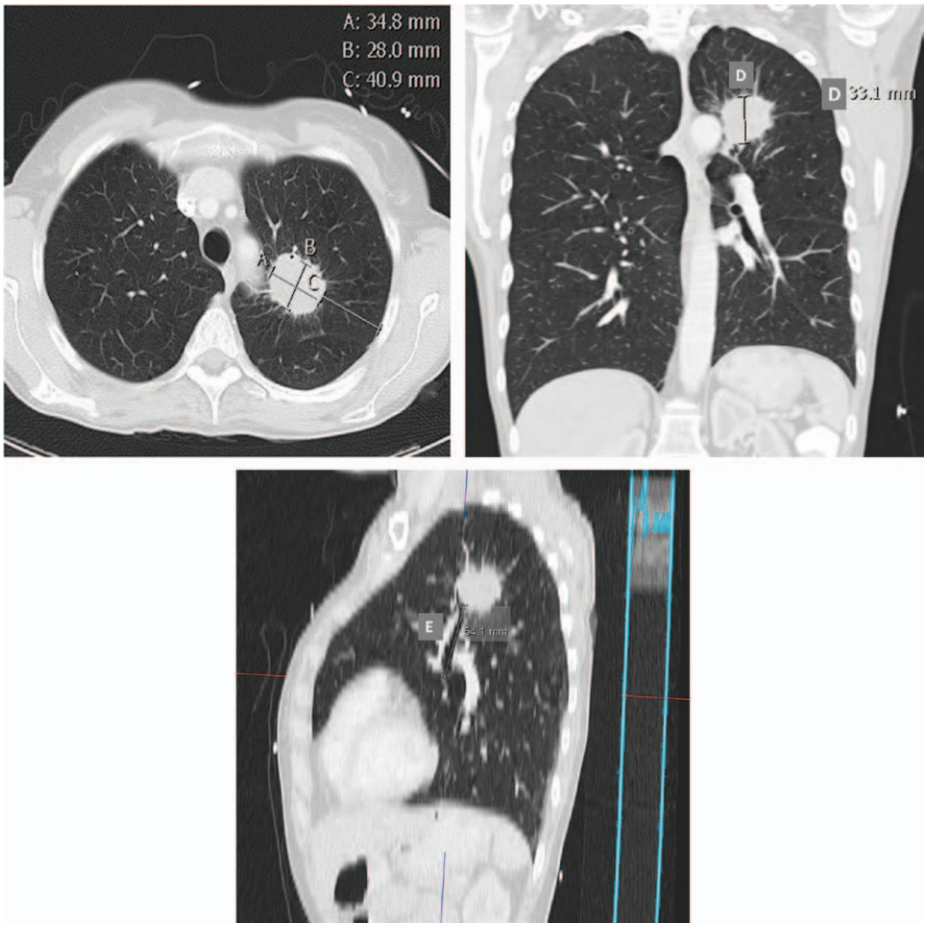

FIGURE 1. The primary tumor is located in segment 2 of the left upper lobe on computed tomography. *A,* The lesion was 34.8 mm in LLD and 28.0 mm in LPLD measured on axial CT images, while located 40.9 mm from the chest wall (Dthorax). *B,* The lesion was 33.1 mm in LAD measured on coronal CT images. *C,* The lesion was located 54.1 mm from the secondary carina (Dcarina) measured by volume viewing software (AGFA HealthCare NV, Mortsel, Belgium). LLD, longest lesion diameter; LPLD, longest perpendicular lesion diameter; CT, computed tomography; LAD, longest apicocaudal diameter.

accessed by randomly passing the rEBUS-MP into the mentally selected (sub)segmental bronchi without fluoroscopic or navigational guidance. After detection of the lesion by the rEBUS-MP, the bronchoscope was kept in place at the nearest visible subsegmental carina and the rEBUS-MP was removed while measuring the distance between the detected lesion and the tip of the bronchoscope. This was considered the 'rEBUS-MP measurement method'. Thereafter, a marked biopsy forceps (single-use Radial Jaw 2.0 mm biopsy forceps, Boston Scientific, USA) was introduced into the target (sub)segmental bronchus for a distance as measured and marked on the forceps, and at least five forceps TBLB were taken for histological analysis[12]. Neither X-ray fluoroscopy- nor EBUS-guided sheath were used.

EBUS-MP-guided TBLB samples were considered diagnostic when a specific histopathological diagnosis was consistent with the clinical presentation and no further invasive diagnosis or follow-up was required. The diagnostic yield was calculated from this assessment. In case of normal findings or a nonspecific inflammation on microscopy, the final specific diagnosis was based on an additional invasive biopsy (percutaneous core needle or surgical biopsy) when appropriate and/or radiologic follow-up of at least 6 months. The diagnostic sensitivity (true positive/(true positive + false negative)) of a TBLB could be calculated from the final specific diagnosis.

Statistical Analysis

Data analysis was performed using SPSS statistical software (IBM SPSS Statistics 20; Chicago, IL). Continuous variables were analyzed using one-way anova, and dichotomous variables were analyzed with Fisher's exact test, as appropriate. A multivariate logistic regression was performed to identify the significant predictors of the diagnostic yield ($p < 0.05$). Multivariate logistic regression was used to identify the independent variables contributing to statistical significance. The OR and associated 95% CI CI were determined to assess the contributions of significant factors. In the multiple logistic regression model, we have used the Variance Inflation Measures to check whether there was multicollinearity for the proposed model. All reported p values were two-sided, and a p value less than 0.05 was considered statistically significant.

RESULTS

Demographics

A total of 760 lesions in 760 patients (490 men and 270 women; mean age 67 years) were examined. A total of 639 (84%) lesions were detected by rEBUS-MP, and a definitive pathological diagnosis was established in 471 (62%) lesions by rEBUS-MP-guided TBLB (Table 1). The lobar location of the pulmonary lesions was variously distributed: 220 in the right upper lobe, 37 in the right middle lobe, 155 in the right lower lobe, 215 in the left upper lobe, and 133 in the left lower lobe (Table 1). The mean ± SD LLD and LPLD on axial CT images were 43 ± 2 and 25 ± 1 mm, respectively. The mean ± SD LAD on coronal CT images and mean ± SD Dthorax on axial CT images were 26 ± 1 and 22 ± 2 mm, respectively. The mean ± SD Dcarina on 3D-CT scan was 55 ± 2 mm. A bronchus sign was present in 618 (81%) lesions. The entire study group consisted of 555 (73%) malignant lesions and 205 (27%) benign lesions (Table 2). The proportion of benign lesions visualized by rEBUS-MP was 77%, but its diagnostic yield of TBLB was only 36%. Benign lesions with a specific diagnosis based on TBLB ($n = 74$) included mainly COP, sarcoidosis, mycobacterial and fungal infection, lymphocytic interstitial pneumonia, hamartoma and Wegener's granulomatosis. The proportion of malignant lesions detected by rEBUS-MP was 87%, and its diagnostic yield of rEBUS-MP-guided TBLB was 72%. A pneumothorax occurred in nine patients (pneumothorax rate 1.2%) of whom one patient required an intercostals catheter drainage.

Univariate Analysis

Univariate analysis of several CT scan characteristics (bronchus sign, lesion location, and lesion size) in relation to the rEBUS-MP visualization yield and guided TBLB diagnostic yield are displayed in Table 1. Bronchus sign was significantly associated with visualization yield and diagnostic yield. EBUS-MP detected 97% of the pulmonary lesions with a bronchus sign on CT scan, and the guided TBLB finally diagnosed 72% of the pulmonary lesions with a bronchus sign. No association was observed between most elements of location (lobar location, segmental location, or Dthorax) and visualization yield, but a statistically significant association was observed between decreasing Dcarina and both visualization and diagnostic yield. The LLD on axial CT images was significantly associated with both visualization and diagnostic yield. The LPLD on axial images and LAD on coronal CT images were strongly associated with visualization and diagnostic yield, but these parameters were strongly correlated with LLD ($r = 0.80$ [95% CI: 0.77–0.83] and $r = 0.78$ [95% CI 0.75–0.81], respectively).

A strong association ($p < 0.001$) was observed between EBUS-MP visualization yield and guided TBLB diagnostic yield. 73% of visualized lesions were diagnosed. Only 2% of undetected lesions were diagnosed. These 2% undetected cases corresponded to two patients in whom a parenchymal bronchial occlusion was assumed as the rEBUS-MP could not be forwarded and therefore TBLB were taken at that distance.

Multivariate Analysis

The result of the multivariate logistic regression analysis indicating significant predictors of the diagnostic yield is depicted in Table 3. Our study identified four factors that directly had a statistically significant impact on the diagnostic yield of rEBUS-MP-guided TBLB: LLD cutoff 20 mm ($p = 0.036$), distance lesion to carina cutoff 40 mm ($p = 0.016$), and segments 1, 3, or 6 ($p < 0.010$, in reference to all other segments). Bronchus sign was the only parameter that indirectly influenced the diagnostic yield through enhancing visualization yield ($p < 0.001$; Fig. 2).

A longest lesion diameter greater than 20 mm was more likely (OR: 1.97) to lead to a definite pathological diagnosis than a LLD less than or equal to 20 mm. A Dcarina greater than 40 mm was less likely (OR: 0.60) to induce a definite pathological diagnosis compared with a Dcarina less than or equal to 40 mm. A pulmonary lesion located in segment 1, 3, or 6 resulted in a significantly higher diagnostic yield compared

with the other segments (OR: 2.32 and $p = 0.002$; OR: 2.28 and $p = 0.004$; OR: 1.93 and $p = 0.009$, respectively).

DISCUSSION

The primary aim of our study was to explore whether CT characteristics can affect the success rate of rEBUS-MP-based evaluation of a bronchoscopically occult pulmonary lesion. Our large retrospective study showed that a LLD greater than 20mm, a distance from lesion to the carina less than or equal to 40 mm, and segmental location (segments 1, 3, or 6) more likely lead to a definitive diagnosis based on rEBUS-MP-guided TBLB. The distance to the secondary or tertiary carina has a direct impact on the number of divisions or bronchial generations, and the size of the lesion has a direct impact on the number of bronchi reaching the lesion. Although these parameters had a direct effect on the diagnostic yield, the presence of a bronchus sign on the CT scan had the highest impact on the diagnostic yield through an increased visualization yield (Fig. 2).

TABLE 1. Univariate Analysis for Visualization and Diagnostic Yield for CT Images Characteristics of Bronchus Sign, Location, and Size

	EBUS-MP Visualization Yield				EBUS-TBLB Diagnostic Yield			
	N	Detected, *n* (%)	Not Detected, *n*	*p* Value	*N*	Diagnostic, *n* (%)	Not Diagnostic, *n*	*p* Value
Patients	760	639 (84%)	121	<0.001	760	471 (62%)	289	<0.001
Bronchus sign								
Absent	142	41 (29%)	101	<0.001	142	29 (20%)	113	<0.001
Present	618	598 (97%)	20		618	424 (72%)	176	
Location								
Lobe				0.413				0.937
Right upper lobe	220	183 (83%)	37		220	166 (76%)	52	
Right middle lobe	37	33 (89%)	4		37	27 (73%)	10	
Right lower lobe	155	137 (89%)	18		155	119 (20%)	35	
Left upper lobe	215	177 (82%)	38		215	161 (28%)	54	
Left lower lobe	133	109 (82%)	24		133	103 (18%)	30	
Segment				0.149				0.017
1	136	107 (79%)	29		136	88 (65%)	48	
2	151	124 (82%)	27		151	88 (58%)	63	
3	109	96 (88%)	13		109	77 (71%)	32	
4 and 5	78	67 (86%)	11		78	41 (53%)	37	
6	143	126 (88%)	17		143	100 (70%)	43	
7 and 8	43	39 (91%)	4		43	26 (61%)	17	
9	44	37 (84%)	7		44	24 (55%)	20	
10	56	43 (77%)	13		56	27 (48%)	29	
DCARINA (mm)				<0.001				<0.001
≤30	136	125 (92%)	11		136	101 (74%)	35	
>30	624	514 (82%)	110		624	370 (59%)	254	
≤40	212	195 (92%)	17		212	157 (74%)	55	
>40	548	444 (81%)	104		548	313 (57%)	234	
≤50	311	282 (90%)	29		311	219 (70%)	92	
>50	449	357 (70%)	92		449	252 (56%)	197	
≤60	426	381 (89%)	45		426	293 (69%)	133	
>60	334	258 (77%)	76		334	178 (53%)	156	
Mean ± SD	All	53 ± 2 mm	67 ± 6 mm	<0.001	All	51 ± 2 mm	61 ± 3 mm	<0.001
DTHORAX (mm)				0.456				0.630
≤0	242	212 (88%)	30		242	159 (66%)	83	
>0	518	427 (82%)	91		518	312 (60%)	206	
≤5	265	229 (86%)	36		265	171 (65%)	94	
>5	495	410 (83%)	85		495	300 (61%)	195	
≤10	301	257 (85%)	44		301	189 (63%)	112	
>10	459	382 (83%)	77		459	282 (61%)	177	
Mean ± SD	All	22 ± 2 mm	24 ± 4 mm	0.456	All	22 ± 2 mm	23 ± 3 mm	0.630

(*Continued*)

TABLE 1. (*Continued*)

	EBUS-MP Visualization Yield				EBUS-TBLB Diagnostic Yield			
	N	**Detected, *n* (%)**	**Not Detected, *n***	***p* Value**	***N***	**Diagnostic, *n* (%)**	**Not Diagnostic, *n***	***p* Value**
Size								
LLD (mm)				<0.001				<0.001
≤10	4	3 (75%)	1		4	2 (50%)	2	
>10	756	636 (84%)	120		756	469 (62%)	287	
≤20	81	46 (57%)	35		81	28 (35%)	53	
>20	679	593 (87%)	86		679	443 (65%)	236	
≤30	243	168 (69%)	75		243	110 (45%)	133	
>30	517	471 (91%)	46		517	361 (70%)	156	
Mean ± SD	All	46±2 mm	29±3 mm	<0.001	All	47±2 mm	36±2 mm	<0.001
LAD (mm)				<0.001				<0.001
≤10	54	32 (59%)	22		54	23 (43%)	31	
>10	706	607 (86%)	99		706	448 (63%)	258	
≤20	324	241 (75%)	83		324	164 (51%)	160	
>20	436	398 (91%)	38		436	307 (70%)	129	
≤30	543	432 (80%)	111		543	308 (57%)	235	
>30	217	207 (95%)	10		217	163 (75%)	54	
Mean ± SD	All	27±1 mm	18±2 mm	<0.001	All	28±2 mm	22±1 mm	<0.001
LPLD (mm)				<0.001				<0.001
≤10	47	26 (55%)	21		47	18 (38%)	29	
>10	713	613 (86%)	100		713	453 (64%)	260	
≤20	326	240 (74%)	86		326	161 (49%)	165	
>20	434	399 (92%)	35		434	310 (71%)	124	
≤30	538	427 (80%)	111		538	305 (57%)	233	
>30	222	212 (96%)	10		222	166 (75%)	56	
Mean ± SD	All	27±1 mm	18±2 mm	<0.001	All	28±1 mm	22±1 mm	<0.001

CT, computed tomography; EBUS-MP, endobronchial ultrasound miniprobe; TBLB, transbronchial lung biopsy; LPLD, longest perpendicular lesion diameter; LAD, longest apicocaudal diameter.

The posthoc aim was to establish an algorithm to approach a pulmonary lesion. As the diagnostic performance of rEBUS-MP-guided TBLB is directly influenced by the lesion location and the lesion size, we divided our entire study cohort into three patient groups based on axial CT images (Table 4). Group 1 represented 'peripheral small' defined as a lesion on CT scan characterized by a Dthorax = 0 mm together with a LLD of less than or equal to 30mm. Group 2 represented 'central small' defined as a lesion on CT scan characterized by a Dthorax greater than 0 mm together with a LLD of less than or equal to 30 mm. Group 3 represented 'any large' defined as a lesion on CT scan characterized by a LLD of greater than 30 mm (Fig. 1). The cutoff at 30 mm for small versus large lesion is based on relevant clinical elements, such as T1 category by the International Association for the Study of Lung Cancer tumor, node, metastasis system, the definition of a solitary pulmonary nodule, and the observed highest differential rate between visualization yield and diagnostic sensitivity. The visualization yield and diagnostic sensitivity of 72 and 57%, respectively, were suboptimal for lesions allocated to group 1 and we might suggest a CT-guided percutaneous core needle biopsy as the preferred invasive diagnostic test based upon a favorable diagnostic yield to pneumothorax ratio[13–14]. The visualization yield and diagnostic sensitivity of 69% and 53%, respectively, were suboptimal for lesions allocated to group 2, but we believe that we can improve the visualization and diagnostic yield by applying modern bronchoscopic techniques (e.g., ultrathin bronchoscope or a guided sheath technique) and/or navigation tools (e.g., virtual bronchoscopy)[15–17]. Finally, we consider a visualization yield and diagnostic sensitivity of 91 and 81%, respectively, acceptable for lesions allocated to group 3 and assessed by a conventional bronchoscope with guided TBLB after a 'rEBUS-MP measurement method'.

It has been established that a strong correlation exists between rEBUS-MP visualization yield and diagnostic yield[6–10, 18–20]. A reported rEBUS-MP visualization yield of 74–93% and diagnostic yield of 58–87% for bronchoscopically occult pulmonary lesions implicates that the visualization yield is 10–20% higher than the diagnostic yield. Our result is in line with this observation, as rEBUS-MP led to visualization of 83% of the pulmonary lesions and a specific diagnosis in 62% of the pulmonary lesions (Table 1). Factors such as sampling error (no guided sheath used; lesion tangential to the bronchus), prevalence of benign disease (which is less likely diagnosed by TBLB alone), and the applied definition of a

TABLE 2. Characteristics of 760 Study Patients Referred for Radial EBUS-MP Bronchoscopy

Final Diagnosis, Characteristics	Proportion of Lesions, *n* (%).	Visualization Yield for rEBUS-MP, *n* (%)	Diagnostic Yield for TBLB, *n* (%)
Malignant lesions	555/760 (73%)	481/555 (87%)	397/555 (72%)
NSCLC	480	419 (76%)	350 (63%)
Adenocarcinoma	245	216 (88%)	189 (77%)
Squamous cell Ca	124	111 (90%)	99 (80%)
NSCLC-NOS[a]	96	78 (81%)	51 (53%)
LCNEC	1	1 (100%)	1 (100%)
AdenoSquamous cell Ca	5	5 (100%)	4 (80%)
Carcinoid	9	8 (89%)	6 (67%)
SCLC	32	30 (94%)	27 (84%)
Meta extrathoracic Ca	37	26 (70%)	15 (41%)
Lymphoma	6	6 (100%)	5 (83%)
Benign lesions	205/760 (27)	158/205 (77%)	74/205 (36%)
Sarcoidosis	19	18 (95%)	12 (63%)
Fungal disease	5	4 (80%)	3 (60%)
COP	38	37 (97%)	30 (79%)
Wegener	5	5 (100%)	2 (40%)
- Other[b]	138	94 (68%)	27 (20%)

[a]Combination of pathological proven NSCLC-NOS and lesions without a pathological proof but suspected for lung cancer and as such treated with radiotherapy based on a multidisciplinary tumor board decision.

[b]Pneumonia (*n* = 8), hamartoma (*n* = 2), mycobacterium species (*n* = 10), lymphocytic interstitial pneumonia (*n* = 5), rheumatoid lung nodule (*n* = 2), extrinsic allergic alveolitis (*n* = 1), meningioma (*n* = 1), solitary fibrous tumor (*n* = 1), and aspecific inflammation (*n* = 108).

n, number; TBLB, transbronchial lung biopsy; NSCLC, non–small-cell lung cancer; NOS, not otherwise specified; LCNEC, large cell neuro-endocrine carcinoma; SCLC, small cell lung cancer; COP, cryptogenic organizing pneumonia; rEBUS-MP, radial endobronchial ultrasound miniprobe.

TABLE 3. Multivariate Logistic Regression Analysis of Factors Leading to a Definitive Diagnosis Based on rEBUS-MP-guided TBLB

Variable	Contrast	B	SE	Odds Ratio	OR 95% CI	*p* Value
LLD	Largest lesion diameter > vs ≤ 20 mm	0.676	0.322	1.965	1.045–3.695	0.036
DCARINA	Dcarina > vs ≤40 mm	-0.509	0.212	0.601	0.397–0.911	0.016
SEGMENT	Segment 1 vs all other segments	0.839	0.275	2.315	1.351–3.967	0.002
	Segment 3 vs all other segments	0.823	0.285	2.278	1.303–3.984	0.004
	Segment 6 vs all other segments	0.657	0.252	1.928	1.177–3.160	0.009
rEBUS-MP	Detected vs not detected	5.054	0.724	156.671	37.90–674.69	<0.001

TBLB, transbronchial lung biopsy; OR, odds ratio; CI, confidence interval; LLD, longest lesion diameter; DCARINA, distance between lesion and carina; rEBUS-MP, radial endobronchial ultrasound miniprobe; SE, standard error..

'specific diagnosis' are suggested factors responsible for this 20% differential yield between visualization and diagnosis.

The major limitations of our study are its retrospective nature and applied methodology. First, we tried to minimize patient selection bias by including all consecutive patients who have undergone a rEBUS-MP investigation at our center between January 2011 and December 2013. It should be stressed that solid lesions less than 10 mm surrounded by lung parenchyma and solid lesions less than 15 mm touching the visceral pleura were excluded for a rEBUS-MP investigation. Second, we adopted a homogenous rEBUS-MP methodology with guided forceps TBLB tissue sampling without using additional auxiliary tools, such as a guided sheath, bronchial brushing or washing, X-ray fluoroscopy, or virtual navigation techniques, which might positively impact on the diagnostic yield. Third, the diagnostic yield of small bronchoscopic TBLB depends on the determined criteria for a specific diagnosis and should not be tenuous. Therefore, the authors did not accept the diagnosis of nonspecific inflammation as a specific diagnosis even when the treating physician decided to follow-up the patient based on the combined TBLB result and clinical features. Fourth, for the primary end point of our study, we decided to evaluate the diagnostic yield instead of the diagnostic sensitivity of rEBUS-MP-guided TBLB. This was decided given the suboptimal negative predictive value of 0.37 (95% CI: 0.31–0.43) for TBLB.

In conclusion, our study revealed that lesion size, distance to secondary or tertiary carina, and segment are significant direct predictors of the diagnostic yield in bronchoscopy occult pulmonary lesions, whereas bronchus sign had a significant impact through an increased visualization yield.

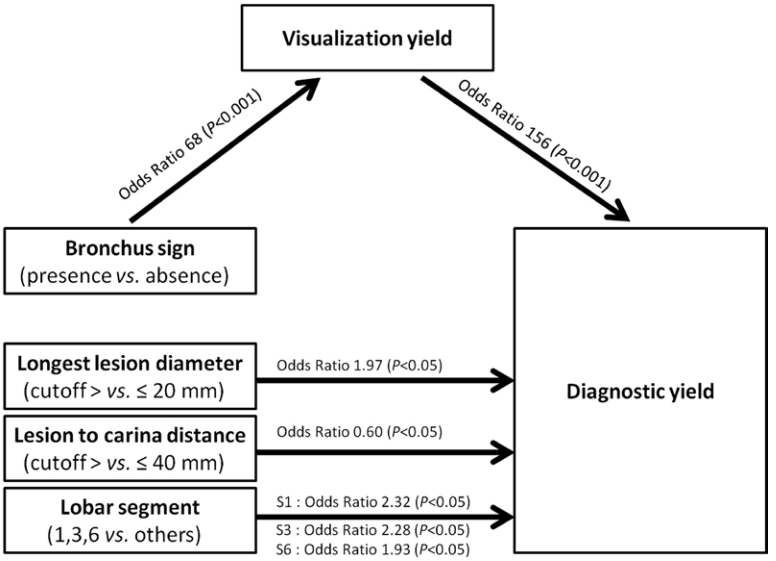

FIGURE 2. Schematic presentation of factors having a significant impact on the diagnostic yield of rEBUS-MP-guided TBLB. TBLB, transbronchial lung biopsy; rEBUS-MP, radial endobronchial ultrasound miniprobe.

TABLE 4. Posthoc Patient Grouping Based on Axial 2D-CT Images

CT characteristics of Pulmonary Lesion	*n* of Patients	Prevalence Malignancy	Visualization Yield	Diagnostic Yield	Diagnostic Sensitivity
Group 1 'peripheral small'	32	69%	72%	50%	57%
Group 2 'central small'	211	71%	69%	45%	53%
Group 3 'any large'	517	74%	91%	70%	81%

CT, computed tomography; *n*, number.

REFERENCES

1. Rivera JO, Ortiz M, González-Stuart A, Hughes H. Initial diagnosis of lung cancer: ACCP evidence-based clinical practice guidelines (2nd edition). *Chest* 2007;132:131S–148S.
2. Baaklini W, Reinoso M, Gorin A, Sharafkaneh A, Manian P. Diagnostic yield of fiberoptic bronchoscopy in evaluating solitary pulmonary nodules. *Chest* 2000;117:1049–1054.
3. Wang Memoli J, Nietert P, Silvestri G. Meta-analysis of guided bronchoscopy for the evaluation of the pulmonary nodule guided bronchoscopy for pulmonary nodules. *Chest* 2012;142:385–393.
4. Steinfort DP, Khor YH, Manser RL, Irving LB. Radial probe endobronchial ultrasound for the diagnosis of peripheral lung cancer: Systematic review and meta-analysis. *Eur Respir J* 2011;37:902–910.
5. Gex G, Pralong J, Combescure C, Seijo L, Rochat T, Soccal PM. Diagnostic yield and safety of electromagnetic navigation bronchoscopy for lung nodules: A systematic review and meta-analysis. *Respiration* 2014;87:165–176.
6. Yoshikawa M, Sukoh N, Yamazaki K, et al. Diagnostic value of endobronchial ultrasonography with a guide sheath for peripheral pulmonary lesions without X-ray fluoroscopy. *Chest* 2007;131:1788–1793.
7. Huang CT, Ho CC, Tsai YJ, Yu CJ, Yang PC. Factors influencing visibility and diagnostic yield of transbronchial biopsy using endobronchial ultrasound in peripheral pulmonary lesions. *Respirology* 2009;14:859–864.
8. Dooms C, Verbeken E, Becker H, Demedts MG, Vansteenkiste JF. Endobronchial ultrasonography in bronchoscopic occult pulmonary lesions. *J Thorac Oncol* 2007;2:121–124.
9. Yamada N, Yamazaki K, Kurimoto N, et al. Factors related to diagnostic yield of transbronchial biopsy using endobronchial ultrasonography with a guide sheath in small peripheral pulmonary lesions. *Chest* 2007;132:603–608.
10. Chen A, Chenna P, Loiselle A, Massoni J, Mayse M, Misselhorn D. Radial probe endobronchial ultrasound for peripheral pulmonary lesions. *Ann Am Thorac Soc* 2014;11:578–582.
11. Naidich D, Sussman R, Kutcher W, Aranda CP, Garay SM, Ettenger NA. Solitary pulmonary nodules: CT-bronchoscopic correlation. *Chest* 1988;93:595–598.
12. Popovich J Jr, Kvale PA, Eichenhorn MS, Radke JR, Ohorodnik JM, Fine G Diagnostic accuracy of multiple biopsies from flexible fiberoptic bronchoscopy. A comparison of central versus peripheral carcinoma. *Am Rev Respir Dis* 1982;125:521–523.
13. Ohno Y, Hatabu H, Takenaka D, et al. CT-guided transthoracic needle aspiration biopsy of small (< or = 20 mm) solitary pulmonary nodules. *AJR Am J Roentgenol* 2003;180:1665–1669.
14. Yeow K, Su I, Pan K, et al. Risk factors of pneumothorax and bleeding: multivariate analysis of 660 CT-guided coaxial curring needle lung biopsies. *Chest* 2004;126:748–754.
15. Ishida T, Asano F, Yamazaki K, et al.; Virtual Navigation in Japan Trial Group. Virtual bronchoscopic navigation combined with endobronchial ultrasound to diagnose small peripheral pulmonary lesions: A randomised trial. *Thorax* 2011;66:1072–1077.
16. Asano F, Shinagawa N, Ishida T, et al. Virtual bronchoscopic navigation combined with ultrathin bronchoscopy. A randomized clinical trial. *Am J Respir Crit Care Med* 2013;188:327–333.
17. Tamiya M, Okamoto N, Sasada S, et al. Diagnostic yield of combined bronchoscopy and endobronchial ultrasonography, under LungPoint guidance for small peripheral pulmonary lesions. *Respirology* 2013;18:834–839.
18. Herth FJ, Eberhardt R, Becker HD, Ernst A. Endobronchial ultrasound-guided transbronchial lung biopsy in fluoroscopically invisible solitary pulmonary nodules: A prospective trial. *Chest* 2006;129:147–150.
19. Paone G, Nicastri E, Lucantoni G, et al. Endobronchial ultrasound-driven biopsy in the diagnosis of peripheral lung lesions. *Chest* 2005;128:3551–3557.
20. Fuso L, Varone F, Magnini D, et al. Role of ultrasound-guided transbronchial biopsy in the diagnosis of peripheral pulmonary lesions. *Lung Cancer* 2013;81:60–64.